Role of Polyelectrolyte Charge Density in Tuning Colloidal Forces

T. Abraham
Bionanomaterials Group, Nanotechnology Research Institute, AIST, Tsukuba Central 5, Tsukuba Science City 305-8565, Japan

D. Christendat, Z. Xu, and J. Masliyah
Dept. of Chemical and Materials Engineering, University of Alberta, Edmonton T6G 2G6, Canada

J. F. Gohy and R. Jérôme
Center for Education and Research on Macromolecules, University of Liège, Sart-Tilman B6, 4000 Liège, Belgium

DOI 10.1002/aic.10255
Published online in Wiley InterScience (www.interscience.wiley.com).

An atomic force microscope was used to study the effects of polymer charge density on surface interactions between similarly charged silica surfaces. Copolymers of acrylamide and acrylic acid of three different charge densities (f_p = 15, 40, and 70%) were used. The dynamic light-scattering technique was used to obtain the characteristic size of these polymers in solution. Flocculation tests were performed to complement force–distance measurement. At 20 mM KCl and pH ~ 8.0, the low charge density copolymer (f_p = 15%) caused a purely repulsive force profile between silica surfaces irrespective of the added polymer concentration, suggesting a strong adsorption of the copolymer on the surface. The medium (f_p = 40%) and high (f_p = 70%) charge density copolymers, on the other hand, provided an adhesive bridging attraction at low polymer concentrations, but a purely repulsive force at higher polymer concentrations. The range of these repulsive forces, however, was significantly smaller than that measured for the low charge density polymer. The medium and high charge densities exhibit nearly an identical behavior in controlling the intersurface forces, although the forces are different with respect to magnitude. The flocculation tests follow the same trend as that of force–distance data, where a complete, a partial, and no flocculation observed with high, medium, and low charge density polymers, respectively. In all the cases, the range of surface interactions can be correlated with the polymer chain dimension corresponding to the fast diffusion process (individual chains) obtained from dynamic light-scattering measurements. Mean-field models proposed for charged polymers can qualitatively explain both the dependency of bridging interactions on polymer charge density and the dependency of force–distance profiles on added polymer concentrations. Finally, a mean-field model was used quantitatively to account for the measured electrosteric interactions and their dependency on polymer charge density. © 2004 American Institute of Chemical Engineers *AIChE J,* 50: 2613–2626, 2004
Keywords: interfaces, colloids, polymer charge density, flocculation

Introduction

Polyelectrolytes and their interfacial characteristics are becoming increasingly important because of their indispensable role in nanostructured and environmentally friendly colloidal systems and in several biotechnology applications (Attia, 1987; Farinato et al., 1999; Texter and Tirrell, 2001). In such situations, the ionic macromolecules play an important role of tuning the surface interactions. One of the most important inherent polyelectrolyte characteristics that control the surface interactions is the polymer charge density (f_p). Polyelectrolyte adsorption, in general, results from competition among various short-range and long-range forces (Borukhov et al., 1999; Lyklema, 1995). Solvation or hydration force between the

Current address of T. Abraham: Dept. of Biochemistry, 3-39 Medical Sciences Buildings, University of Alberta, Edmonton, Canada T6G 2H7; e-mail: tabraham@ualberta.ca.
Correspondence concerning this article should be addressed to J. Masliyah at jacob.masliyah@ualberta.ca.

surface and the solvent (water), the intra- and interelectrostatic repulsion among charged polymer units and so forth act against polymer adsorption. Polyelectrolyte adsorption, however, is facilitated by electrostatic attraction between those polyelectrolyte segments and surface carrying opposite charges, van der Waals forces, specific interactions between polyelectrolytes and surface sites such as hydrogen bonding, and poor solvent environment induced by screening of the polyelectrolytes charges because of added salts. In addition, the polyelectrolyte adsorption is favored by attachment of multisegments, the release of counterions from both surface and polyelectrolyte chains, and the low diffusion of chains near the surfaces. However, the adsorption process leads to a loss of entropy as a result of the confinement of the chains on the surfaces.

There has been a considerable theoretical effort to understand polyelectrolyte adsorption and the resulting surface interactions. The main theoretical tools include analytical mean-field models (Borukhov et al, 1999; Joanny and Chatellier, 1996, 2000; Pincus, 1991; Podgornik, 1991, 1992; Podgornik et al., 1995; Zhulina and Borisov, 1997) and molecular simulations (Dahlgren et al., 1993; Linse, 1996; Podgornik et al., 1995; Shubin and Linse, 1998). Studies with these models showed that the structure of the adsorbed layer and resulting surface interactions are strong functions of polymer charge density, surface potential or surface charge density, nonelectrostatic polymer–surface interactions, concentration of added salts, and other relevant system characteristics such as the quality of solvent and solution pH. On the experimental side, systematic investigations evaluating the influence of these factors are few (Abraham et al., 2000, 2001; Biggs, 1995; Dahlgren, 1994; Dahlgren et al., 1993; Kamiyama and Israelachvili, 1992; Kelley et al., 1998; Lowack and Helm, 1998; Osterberg et al., 2001).

The adsorbed polyelectrolyte layers and the nature of interactions as a function of polymer charge density have been studied in only a few cases (Dahlgren et al., 1993; Osterberg et al., 2001). Dahlgren et al. (1993) investigated interactions between mica surfaces in the presence of random copolyelectrolytes of two different low charge fractions (f_r), AM–CMA-10 ($f_r = 0.1$) and AM–CMA-30 ($f_r = 0.3$), which were prepared using different ratios of neutral acrylamide (AM) segments and positively charged (2-acryloxy ethyl) trimethyl ammonium chloride (CMA) segments. In this case, the positively charged CMA segments and negatively charged mica surface interact electrostatically and at the same time AM segments interact with mica surface by hydrogen bonding. At low charge density ($f_r = 0.1$), the repulsive interactions were dominant, whereas for the higher charge fraction polymers ($f_r = 0.3$), an attractive force was observed at distances of surface separation below about 10 nm. In a closely related study, Osterberg et al. (2001) studied the interactions between mica surfaces in the presence of two different xylans of relatively low charge densities, one with 0.5% of the segments carrying carboxylic acid groups and the other with 9% of the segments having carboxylic groups. They found that the xylan with 9% of the segments containing carboxylic groups showed slightly more long-range repulsion than xylan with 0.5% charged groups. To date, a systematic study on the role of linear charge density of polyelectrolyte systems using wide range of charge densities (f_p) has not been carried out. The main goal of the present investigation is to compare high molecular weight polyelectrolytes of three different charge densities in terms of their adsorption on a solid surface and subsequent surface interactions in such systems. In this study we used random copolymers, which were prepared using different ratios of simple neutral acrylamide and negatively charged acrylic monomers. Three carefully chosen charge densities (that is, $f_p = 15$, 40, and 70%, representing a broad range of charge densities) were used under similar experimental conditions (Figure 1). Here, the charge density f_p is defined as the weight percentage of acrylic acid in the polyelectrolyte polymer. To obtain a more comprehensive overview, the results were tested with currently available mean-field models proposed for similar systems. This endeavor aims to extend our current understanding of the role of polyelectrolyte charge densities on conformational and interaction properties at interfaces.

Experimental

Materials

High molecular weight random anionic copolymers, composed of different ratios of simple neutral acrylamide segments and negatively charged acrylic segments (referred to as AMAC hereafter), were synthesized by free-radical polymerization. Three different charge densities (f_p), AMAC-15, AMAC-40, and AMAC-70, which contain 15, 30, and 70 wt% acrylic segments, respectively, were synthesized. These copolymers are neutral-charged random copolymers, in which the charged blocks carry negative charges.

In a typical polymerization experiment, 1.5 g of acrylic acid and 8.5 g of acrylamide were dissolved in 10 mL of water. The mixture was degassed by two freeze–thaw cycles. Then, 5 mg of $K_2S_2O_8$ was added and the mixture was heated to 70°C for 24 h. Completion of the polymerization process was indicated by gelation of the polymerization media. The gel was diluted in pure water and purified by dialysis against regularly replaced pure water for 3 days (Spectra-Por membranes, cutoff: 6000–8000 daltons) to remove the unreacted monomers. The polymer was finally recovered by lyophilization of the dialyzed solution. The yield of the polymerization reaction was determined by weighing the collected polymer and was found in all cases to be near 100%. It can thus be ascertained that the copolymer composition is similar to the initial feed of the two comonomers. The synthesized copolymers were characterized by size-exclusion chromatography in buffered water. A Waters apparatus (Waters Associates, Milford, MA), calibrated with poly(acrylic acid) standards, was used. In all cases, the molecular weight of the copolymer was high ($M_n \sim 200{,}000$) and a broad polydispersity index (PDI $\sim$ 3) was noted. The molecular weight characteristics of all three synthesized copolymers are listed in Table 1.

Potassium chloride (KCl; Sigma ultrapure grade) and sodium hydroxide (NaOH, 99.9+ purity) were purchased from Sigma-Aldrich (Canada). Silicon wafers of 1-0-0 crystal planes were purchased from MEMC Electronic Materials (Italy). Silica spheres (colloidal probes) were obtained from Bang Laboratory (Fishers, IL). For flocculation studies, silica particles of 5 μm size were purchased from US Silica (Berkeley Springs, WV). In all experiments, Millipore water (Millipore, Milford, MA) of resistivity 18.2 MΩ cm^{-1} was used as an aqueous medium.

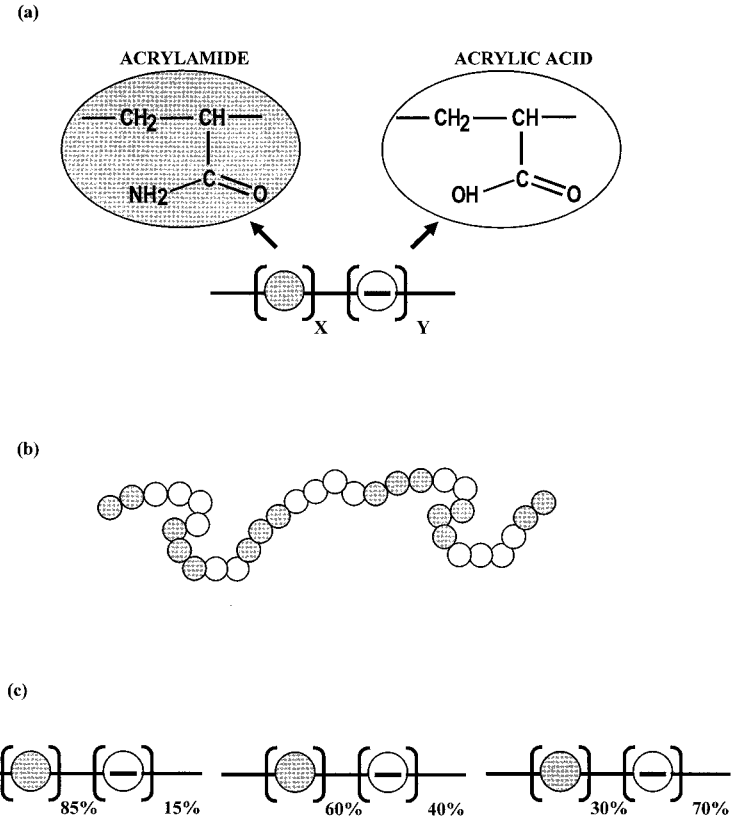

Figure 1. (a) Chemical structure of acrylamide and acrylic acid monomers; (b) a polymer chain showing randomness of monomer units (gray and blank circles represent acrylamide and acrylic acid monomers, respectively); (c) copolymers of three different charge fractions used in this study.

Methods

Force-Measuring Technique. A Nanoscope E atomic force microscope (AFM) from Digital Instruments (Santa Barbara, CA) was used in the force measurements. Gold-coated silicon nitride cantilevers used in the AFM experiments were also obtained from Digital Instruments. Lever-type cantilevers (100 μm wide with spring constants of 0.58 N/m) were used for the force measurements. Cantilevers were modified for the force measurements by attaching a colloidal probe (silica spheres) at the apex of an AFM cantilever using an extremely small quantity of epoxy resin. The scanning electron microscopy (SEM) micrograph indicated that the glue was always confined to the interface between the sphere and the cantilever. The radius of the spheres used in each of the experiment was also obtained from the SEM micrograph.

A detailed description of the use of the AFM in force-measuring mode is provided elsewhere (Abraham et al., 2002; Ducker et al., 1992). Briefly, the surface is approached toward the colloid probe, and the deflection of the cantilever of known spring constant under the influence of the approaching surface is measured using a laser reflected off the cantilever onto a position-sensitive split photodiode. The onset of the constant compliance region is defined as "zero" separation distance, where the deflection of the cantilever is linear with respect to the approaching surface displacement. Surface separation is then estimated from the displacement of the lower surface relative to this constant compliance region. Although there may have been polymer sandwiched between the probe and the surface, the layer thickness under this condition does not change, so that the separation can be considered constant. There was no possible way to determine the absolute separation (and thus the layer thickness) or the contact area. However, this does not alter the form of the interaction and the interpretation of the results. The force (F) acting between the probe and the surface is simply determined from the deflection of the cantilever by using Hooke's law, $F = kx$, where x represents the deflection and k is the spring constant of the cantilever. The measured force was normalized by probe radius for quantitative comparison. In our force measurements, the scatter in force–distance data, especially below 0.05 mN/m, was way too high to make any solid judgment in terms of determining the range of interactions. Therefore, we used 0.05 mN/m as a cutoff value in determining the range of interaction, below which the force was assumed to be zero.

Table 1. Molecular Weights, Polydispersity Indices, and Dimensional Characteristics of Copolyelectrolytes*

Sample	Acrylic Acid (wt %)	M_n	PDI	$\langle R_0^2 \rangle$ (nm)	R_{FL} (nm)
1	15	234,000	3.0	46	822
2	40	176,000	3.1	57	616
3	70	182,000	2.5	58	635

*See text for details.

All solutions involved in the force measurements were prepared with Millipore water of resistivity 18.2 MΩ cm^{-1}. Stock solutions of AM–AC at a concentration of about 200 ppm were prepared 1 week before the experiment. The salt solutions were prepared at least 1 day before the experiments. Force measurements were performed in a solution cell where the colloidal probe (silica sphere) interacts with a flat hydrophilized silicon wafer in an aqueous solution under different experimental conditions. The hydrophilized silicon slides were prepared as follows. Silicon wafers were cut into rectangular pieces. The slides were then cleaned with dichloromethane in an ultrasonic bath for 15 min at about 50°C to remove possible organic surface contaminants. Afterward the wafers were rinsed with Millipore water. This was followed by a cleaning step in an oxidation bath with a mixture of H_2O_2, NH_3, and water at 75°C for about 30–45 min. After rinsing thoroughly with Millipore water, the slides were dried with clean nitrogen. This treatment rendered the surface hydrophilic by generating silanol groups (Si–OH). Unless otherwise stated, all force measurements were conducted after an incubation time of 30 min at room temperature (22 ± 1°C) in a solution of pH ~ 8.0 containing 20 mM KCl. We did not see any significant changes in the force profiles even after 1 h of incubation. Therefore, our system can be considered as in equilibrium after 30 min of incubation time.

Dynamic Light Scattering (DLS). DLS measurements were performed with a Malvern 4700C apparatus equipped with a Malvern 7032 digital correlator and an Ion Laser Technology argon laser with a wavelength of 488 nm. Each DLS datum resulted from the averaging of ten measurements. The scattering angle used for the measurements was 90°. A temperature-controlled refractive index matching bath surrounded the scattering cell. All the measurements were performed in a 20 mM KCl solution at 25°C. The pH was set to 8 by adding the minimum amount of KOH.

The second-order correlation function $G_2(t)$ was measured. In the case of single-exponential decay, $G_2(t)$ can be expressed by the following equation

$$G_2(t) = B[1 + \beta \exp(-2\Gamma t)] = B[1 + \beta|G_1(t)|^2] \quad (1)$$

where B is the baseline, β is an optical constant that depends on the instrument, Γ is the decay rate for the process, t is time, and $G_1(t)$ is the first-order correlation function. Γ is given by

$$\Gamma = Kq^2 \quad (2)$$

where K is the translation diffusion coefficient and q is the absolute value of the scattering vector, and is given by

$$q = [4\pi n \sin(\theta/2)]/\lambda \quad (3)$$

where n is the refractive index of the solvent, θ is the scattering angle, and λ is the wavelength of the incident light. The diffusion coefficient (K) for spherical particles is related to the hydrodynamic diameter (D) by the Stokes–Einstein equation

$$K = k_B T/3\pi\eta D \quad (4)$$

where k_B is the Boltzmann constant, T is the absolute temperature, and η is the viscosity of the solvent. The experimental correlation function was analyzed using CONTIN routines (Provencher, 1979). This program allows the diffusion coefficients and relaxation time distributions to be obtained.

Flocculation Tests. Silica dispersion of 4.8% (w/w) was prepared from 5 μm silica and Millipore water. The settling measurements were performed in the pH range from 7.5 to 8.3 and at 20 mM KCl. The tests were carried out in 50-mL graduated cylinders at room temperature (22 ± 2°C). Polymer solutions of known concentration were added and the cylinders were inverted several times to ensure thorough mixing. The solid–liquid interface or the volume occupied by silica-rich bottom layer, which signifies the extent of flocculation, was recorded after 10 min and overnight. The amount of polymer required to induce flocculation was noted for each polymer.

Anionic copolyelectrolytes

Relevant Characteristics. Poly(acrylamide-*co*-acrylic acid) is an anionic copolymer, whose charge density depends on the pH of the solution. The dimension of the chain is a function of monomer size, number of monomer units, pH, and added salt concentration. Addition of a monovalent salt screens or reduces the electrostatic interaction between the polymer charges and reduces the solvent quality of the polymer backbone, which in turn causes shrinkage of the chains. There are various models developed for predicting the effects of added salt on the conformational properties of polyelectrolyte chains (Fleer et al., 1993). We adopt here a length scale based on the persistence length (Abraham, 2002). Accordingly, mean square end-to-end distance $\langle R_0^2 \rangle$ is

$$\langle R_0^2 \rangle = 2aN\left[l_0 + \frac{l_B}{4l_{eff}^2}\left(\frac{1}{\kappa}\right)^2 \right] \quad (5)$$

where a is the monomer size, N is the number of monomer units, l_0 is the persistence length in the absence of electrostatic interactions, l_B is the Bjerrum length, $1/k$ is the Debye length, and l_{eff} is the effective distance between neighboring charges. For high charge density polyelectrolytes, $l_{eff} = zl_B$, where z is the valency of monomer charge and for low charge density; and $l_{eff} = I_E$, the actual distance between the charges. For the current systems, the pH of the solution was maintained at >8.0, under which the polyelectrolyte is completely dissociated. At 20 mM added divalent salt concentration, the estimated chain dimension $\langle R_0^2 \rangle$ values of all three copolyelectrolytes are given Table 1. Note that the effective distance between the charges (l_{eff}) becomes Bjerrum length (l_B) when the actual distance between charges (l_E) is less than the Bjerrum length (l_B). In addition, one may calculate the fully extended chain length R_{FL} from the equation

$$R_{FL} = aN \quad (6)$$

The calculated R_{FL} values of all the three copolyelectrolytes are also reported in Table 1.

Results and Analysis

Copolymer solution properties

A strong dependency of hydrodynamic diameter as a function of AMAC-15 concentration was observed (Figure 2).

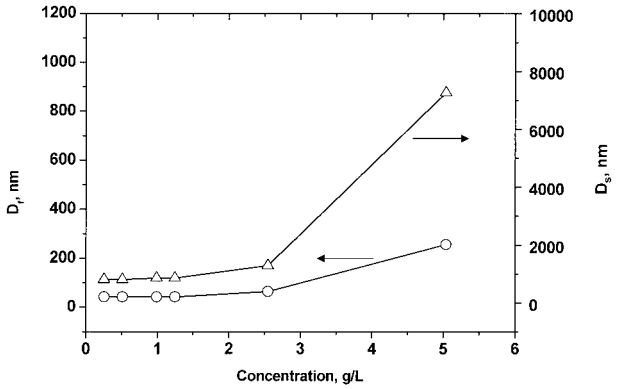

Figure 2. Fast-mode hydrodynamic diameter (D_f) and slow mode (D_s) hydrodynamic diameter as a function of AMAC-15 concentration.

Keys: (△) fast mode; (○): slow mode.

Clearly two regimes can be distinguished: a regime below 3.0 g/L, where the concentration dependency of hydrodynamic dimension is weak, and a regime above 3.0 g/L, where the concentration dependency of hydrodynamic dimensions is strong. For both regimes, a "slow" and a "fast" relaxation mode are observed. This could be attributable to the polyelectrolyte behavior of the copolymer. In salt-free or low salt concentration polyelectrolyte solutions, this feature is commonly observed (Förster et al., 1990). The fast mode (D_f) and slow mode (D_s) hydrodynamic diameters can be attributed to individual polymer chains and polymer aggregates, respectively (Förster et al., 1990). Figure 3a shows the two relaxation modes for the AM–AC-15 at 0.5 g/L. The CONTIN size-distribution histogram shows that the "fast" relaxation mode is predominant over the "slow" relaxation mode (Figure 3b). Table 1 features fast-mode (D_f) and slow-mode hydrodynamic diameters (D_s) determined by the extrapolation of data in the regime below 3.0 g/L to zero copolymer concentration. The measured fast-mode hydrodynamic diameters (D_f) are comparable to the predicted mean square end-to-end distances $\langle R_0^2 \rangle$, although the predicted values are numerically ($\sim$ 20–35%) higher than experimentally measured values. It should be noted that the scattered intensity was low for each experiment. This suggests that these aggregates have rather loose, open structures and must not be considered as micelles with a dense core. The measurements were performed at pH = 8, where the majority of carboxylic acid units are ionized into carboxylates. Hydrogen bonding between acrylamide and acrylic groups could play an important role in the formation of loosely aggregated species. The structure of the investigated copolymer is indeed comparable to statistical polyampholytes (Kujawa et al., 2001).

Forces between silica surfaces in 20 mM KCl

In Figure 4 and inset, we show the measured forces (rectangles) between two silica surfaces in an aqueous solution containing 20 mM KCl at pH $\sim$ 8.0. The measured forces were purely repulsive but of short range, commencing at a distance less than 10 nm, as shown in the insert of Figure 4. The forces can be very well described by DVLO (Derjaguin–Landau–Verwey–Overbeek) theory with a constant surface charge density boundary condition (Israelachvili, 1992; Verwey and Overbeek, 1948). The DLVO forces are the sum of a repulsive electrical double-layer force calculated from the exact Poisson–Boltzmann equation using a numerical solution and a nonretarded van der Waals attraction. The fitted surface charge density and decay length are found to be 0.0053 C/m^2 (that is, charge/30.2 nm^2) and 2.3 nm, respectively. A Hamaker constant of 1.92×10^{-20} J was used (Cappella and Deitler, 1999). DLVO theory predicts that the attractive van der Waals component exceeds double-layer forces at very small distances of separation (2–3 nm). However, the measured forces do not show any attractive component at very small separation distances. This effect has been reported previously by many others, and has been attributed to hydration forces (Israelachvilli, 1992a). The results and the fitted values are in good agreement with several currently reported data available in the literature (Cappella and Deitler, 1999).

Forces between silica surfaces in AMAC-15 solutions

The measured forces between two silica surfaces in an aqueous solution containing 20 mM KCl/pH $\sim$ 8.0 at different polyelectrolyte concentrations are shown in Figure 4. There is little or no change in force profiles (with reference to 20 mM KCl/pH $\sim$ 8) with the polyelectrolyte concentration ranging from 0.1 to 0.5 ppm. When the concentration was increased to 1.0 ppm, a repulsive force extending up to about 30 nm ($0.9D_f$) was observed. The range of interaction is comparable to the chain dimension that corresponds to a fast diffusion process (D_f). On retraction, the force remained repulsive. A further

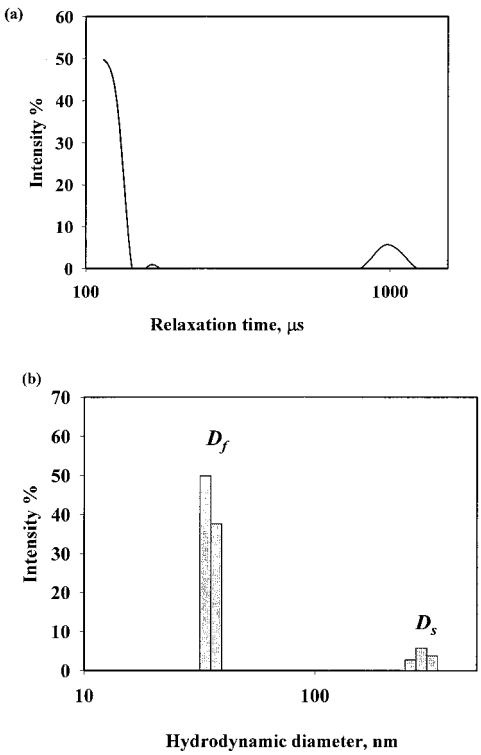

Figure 3. (a) Relaxation times distribution calculated with the CONTIN routine for AMAC-15 at concentration (*C*) of 0.5 g/L. (b) CONTIN size distribution for AMAC-15 at *C* = 0.5 g/L.

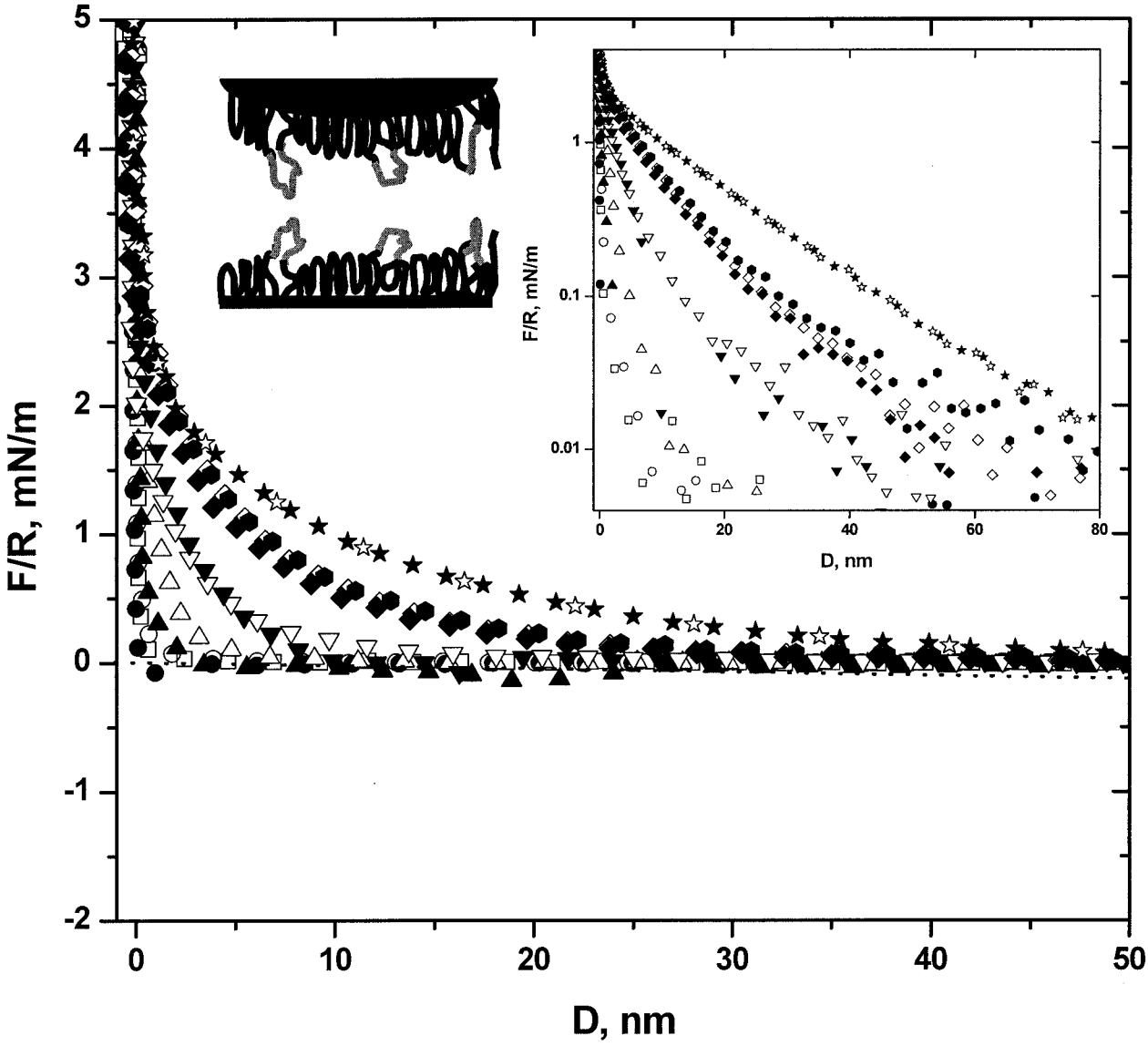

Figure 4. Measured forces (*F/R*) as a function of distance of separation (*D*) between two silica surfaces in an aqueous solution containing 20 mM KCl at pH ~ 8.0 at various AMAC-15 concentrations.

Inset shows force profiles on semilog plot. Open and filled symbols represent approach and retraction, respectively. Keys: (□) 0; (○, ●) 0.1; (△, ▲) 0.5; (▼, ▽) 1.0; (◆, ◇) 5.0; (●, ○) 10.0; and (☆, ★) 50.0 ppm AMAC-15.

increase in polyelectrolyte concentration to 5.0 ppm increased the range of interaction to about 60 nm ($\sim 1.8D_f$), as shown in the insert of Figure 4, and the magnitude of the force became more repulsive. A further tenfold increase of polyelectrolyte concentration (50 ppm) resulted in a force profile that is strongly repulsive, with a range of interaction extending to about 80 nm ($2.4D_f$). The force profiles remained the same when the polyelectrolyte concentrations were further increased. This suggests a surface saturation reached a 50 ppm polyelectrolyte concentration. We note here that, even at these concentrations, the measured ranges of interactions are far below the polyelectrolyte aggregate dimension (D_s). This observation suggests that the polyelectrolyte aggregates possible present in the system do not take part in the adsorption process.

The results, in general, suggest that AMAC-15 adsorbs on silica surfaces for given ionic conditions and adsorption density depends on the bulk AMAC-15 concentration. Such concentration-dependent adsorptions give rise to thick adsorbed polymer layers on silica surfaces, thereby causing strong electrosteric repulsive forces between the surfaces. Note that, in the case of polymers, the relationship between the range of interaction and the adsorption density (or surface density) is well established both theoretically and experimentally (De Gennes, 1987; Israelachvili, 1992b; Milner, 1991). The buildup or crowding of polyelectrolyte molecules at the surfaces stretches the adsorbed layers normal to the surface attributed to the osmotic interaction among the chains, which may give rise to a long-range steric force compounded with electrostatic force. This eventually leads to a longer range of surface interactions at higher polyelectrolyte concentrations.

Presumably, the adsorption is driven by nonelectrostatic factors, that is, hydrogen bonding interaction between amide

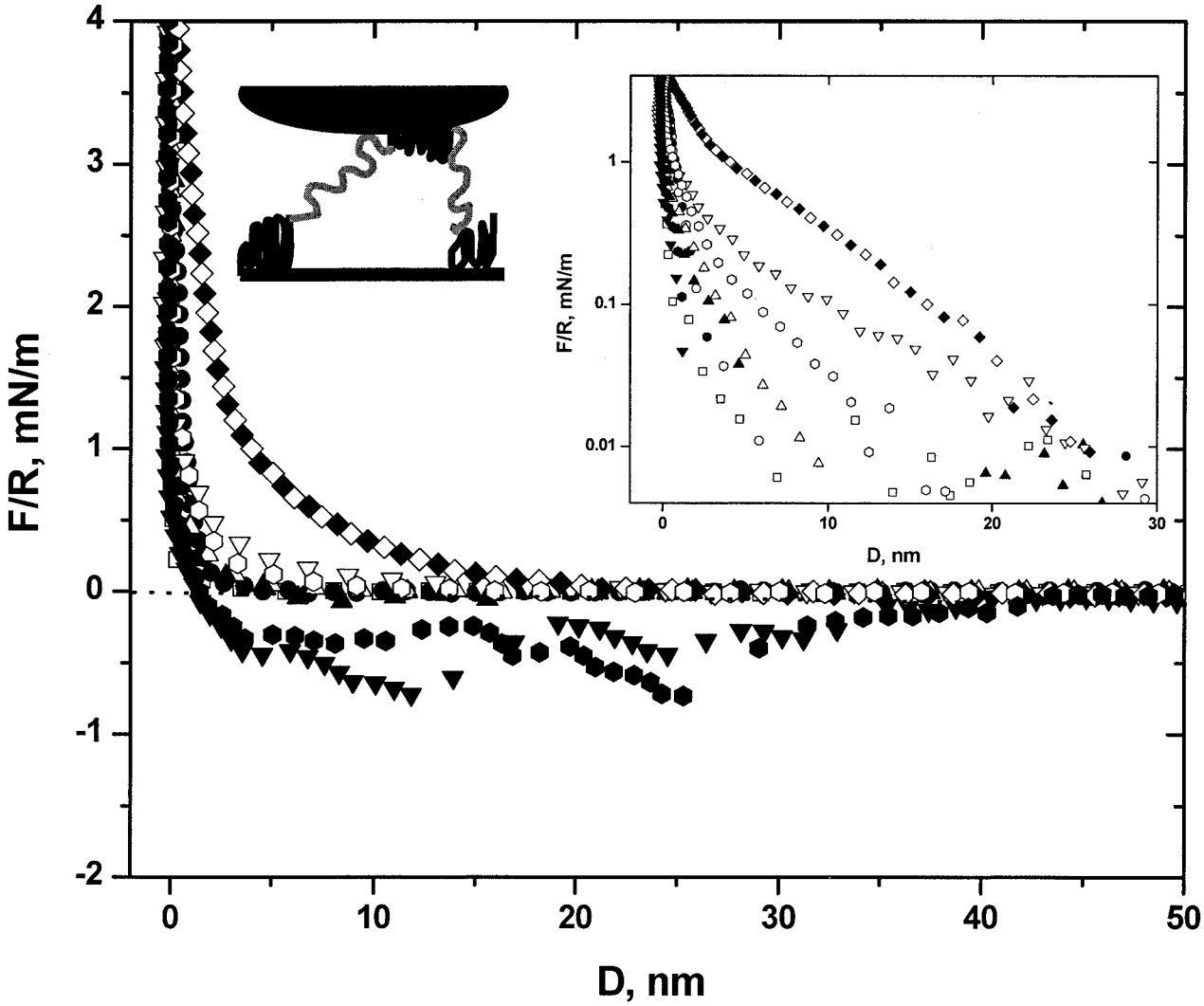

Figure 5. Measured forces (*F/R*) as a function of distance of separation (*D*) between two silica surfaces in an aqueous solution containing 20 mM KCl at pH ~ 8.0 at various AMAC-40 concentrations.

Inset shows force profiles on semi-log plot. Open and filled symbols represent approach and retraction, respectively. Keys: (□) 0; (△, ▲) 0.2; (●, ○) 5.0; (▼, ▽) 10.0; and (◆, ◇) 50.0 ppm AMAC-40.

groups of polymer chains and silanol groups of silica surface. Such a strong adsorption would be expected, considering that the weight fraction of the total monomer units that contain amide groups in AMAC-15 is 85%. Because the charge density (f_p) of AMAC-15 is only 15%, the intra- and interchain electrostatic interactions, a factor that acts against adsorption, is considerably weak. In his mean-field lattice model calculations, Linse (1996) considered the case of favorable nonelectrostatic interactions and predicted increased adsorption with increasing favorable nonelectrostatic interactions.

Forces between silica surfaces in AMAC-40 solutions

In Figure 5, we show measured forces between silica surfaces in 20 mM KCl aqueous solution of pH ~ 8 containing different amounts of AMAC-40. The addition of polyelectrolyte, ranging from 0.2 to 2.0 ppm, caused little or no change in force profiles, suggesting the absence of polymer adsorption. When the polyelectrolyte concentration was increased to 5 ppm, a marginal repulsive force, commencing at about 20 nm (0.4 D_f), was observed as the silica probe approached the substrate. On retraction, the silica probe appeared to roll over the substrate before releasing from the substrate, suggesting adhesive interactions between the surfaces upon contact. The probe followed the surface without any apparent deviation down to 0 mN/m (equilibrium position). Beyond this position, the cantilever parted slightly from the surface to 3.5 nm and an interaction energy of −0.3 mN/m was measured. The interaction energy remained roughly constant until the probe finally released at about 40 nm. No further interaction was measured. This force profile suggests some form of an adhesive interaction between the surfaces upon contact, signifying the formation of polymer bridges across the surfaces. In this case, the data suggest that there is only a partial coverage of the surface by the polymer. Although there could be a layer of polymer on the two surfaces, some free surfaces are still available for polymer adsorption. For this reason, as the surfaces approach

each other, there ought to be a bridging adhesion effect where the dangling tails of the polymers on one surface can contact and be adsorbed onto the other surface, thus potentially exerting an attractive influence when separating two surfaces. Increase of polyelectrolyte concentration to 10 ppm slightly increases the range of repulsive force to about 25 nm on approach, but on retraction a similar adhesive bridging force is observed. Here, again, the probe remains attached in the adhesive regime as described above. A further increase of polyelectrolyte concentration to 50 ppm turns the force profiles to purely repulsive on both approach and retraction, but the magnitude and range of interactions are significantly lower compared to those of the case of 50 ppm AMAC-15 addition under similar conditions.

Force profiles for AMAC-40 are in general very different from those obtained in the presence of AMAC-15. It is evident that the AMAC-40 has less affinity than AMAC-15 to the negatively charged silica surface. In the case of AMAC-40, the adsorbed amounts are lower compared to those of AMAC-15. In AMAC-40, 40 wt % of the total monomer units are charged. However, in AMAC-15, the weight fraction of the charged monomer units is only 15%. This difference can have two consequences. First, AMAC-40 have more expanded conformation structure because of the intrachain electrostatic repulsion; therefore the adsorbed chains occupy more surface area, which in turn leads to a reduced surface density. Second, the interchain electrostatic interaction among polyelectrolyte chains reduces the adsorption density attributed to the repulsion among the chains. Thus, AMAC-40 gives a partial surface coverage at low added polymer concentrations that eventually causes strong bridging attraction between the surfaces. Again, at higher concentrations of AMAC-40, a lower number of chains are adsorbed because of their expanded conformation and electrostatic interactions.

Forces between silica surfaces in AMAC-70 solutions

The measured forces between two silica surfaces in an aqueous solution containing 20 mM KCl and pH $\sim$ 8.0–9.0, at various AMAC-70 concentrations, are shown in Figure 6. As in the case of AMAC-40, there is little or no change in the force profiles with the addition of AMAC-70 at a concentration range of 0.2 to 2.0 ppm. Increase of the polymer concentration to 5.0 ppm caused a jump from a separation distance of about 20 nm into some kind of contact at about 15 nm. From there, the forces remained constant or rose slightly to a separation distance of about 8 nm and then increased monotonically to hard wall contact. On retraction, a large adhesive bridging force was observed. The probe remained attached to the surface up to an adhesive force of 1.85 mN/m. Then, the probe separated very slightly from the surface at this energy level up to a separation distance of about 50 nm and it gradually released to its equilibrium position at about 270 nm. The situation is similar to a partial coverage (and thus polymer bridging adhesion) case outlined in the previous section but with an adhesive energy of a higher magnitude. For the 10 ppm AMAC-70 concentration case, on approach there was no detectable attraction. A repulsive force below about 10 nm monotonically increased to a hard wall contact. On retraction, however, the force decayed (same as on approach) with the two surfaces remaining in contact before they began to separate at about 10 nm. As the surfaces continued to separate, a maximum adhesion force of 0.4 mN/m at 50 nm was measured. The surfaces then slowly separate before finally relaxing at a separation of 40 nm. A further increase in AMAC-70 concentrations to 50 ppm gave purely repulsive forces on both approach and retraction and the measured forces are reversible in the measured range of interactions. The measured force profiles, in general, closely resemble those observed for AMAC-40. The measured adhesive bridging force is, however, of a higher magnitude.

Flocculation

Settling tests on silica dispersion (4.8% w/w, 20 mM KCl, pH 7.5–8.3) were conducted with the three polymers at concentrations ranging from 1 to 100 ppm. It was found that 20 ppm level shows the most contrasting results. Figure 7 shows photographs of silica suspensions at 20 ppm polymer concentration taken after 10 min of settling time. These photographs compare the volumes of silica-rich bottom sediment layer for the three different polymers. A silica-rich layer is clearly seen in the case of the high charge density polymer, AMAC-70. The other two polymers, AMAC-15 and AMAC-40, do not show any settling enhancement. It is evident that a relatively faster settling rate can be accomplished with AMAC-70. Comparison after overnight settling clearly shows the difference among three charge density polymers (Figure 8); a clear silica–water interface is seen in the case of AMAC-70, silica-rich bottom layer is seen for AMAC-40, but still no settling enhancement with AMAC-15. Clearly, at this ppm level, AMAC-40 and AMAC-70 give partial polymer coverage on the silica particle surfaces. This eventually causes silica particles to flocculate through possible bridging interactions. It is also interesting to note the difference in the clarity of the supernatant water obtained for AMAC-70 and AMAC-40. AMAC-70 yields a very clear supernatant water, whereas AMAC-40 gives only partially clear supernatant water where silica particles are still in suspension. This difference can be explained as follows. Compared to AMAC-40, the high charge density polymer AMAC-70 has a relatively expanded conformation. This expanded chain structure may provide an ability to capture more particles (that is, a high capture efficiency. This may lead to the flocculation of most or all the silica particles, which eventually gives rise to a very clear supernatant water. The difference among the three charge density polymers, with respect to causing flocculation of silica/water dispersion, is evident and convincing. Clearly, 20 ppm AMAC-70 is efficient to cause a complete phase separation of silica/water dispersion. As such, the flocculation tests show that a fast and complete flocculation can be accomplished with the high charge density polymer at a low polymer concentration. The sediment height of a flocculated suspension serves as an independent measure of compactness of the formed flocs. As indicated by the arrows in Figure 8, the sediment height of 8 mm for AMAC-40 flocculated suspension is lower than 11 mm for the case of AMAC-70 flocculated suspension, indicating a looser structure of aggregates formed by AMAC-70. The larger interparticle distance for AMAC-70 flocculated aggregates than that for AMAC-40 flocculated aggregates observed in the flocculation test suggests a less-compressible bridge of the flocculant. The larger interparticle distance for AMAC-70 flocculated aggregates than that for AMAC-40 flocculated aggregates observed in the

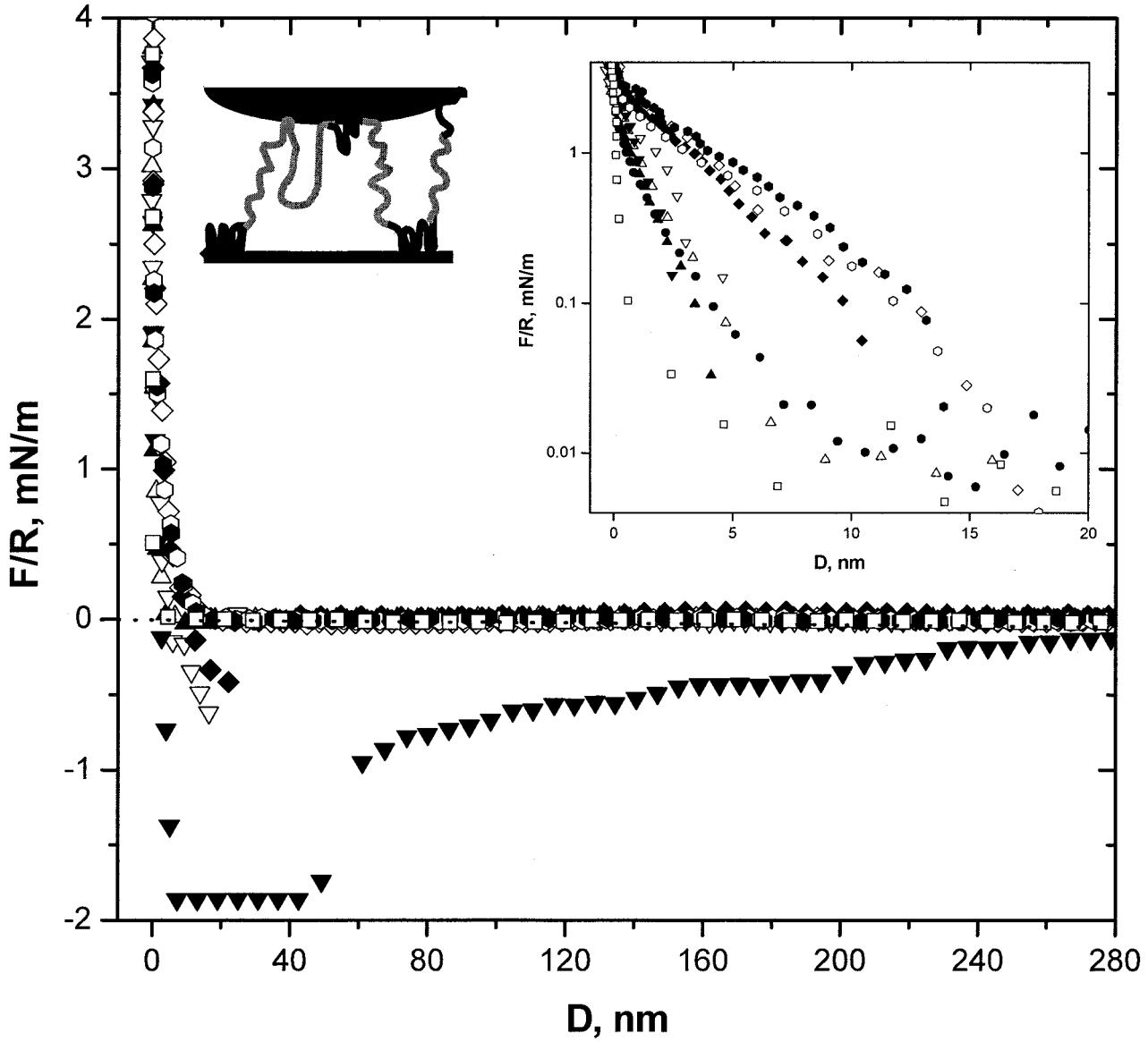

Figure 6. Measured forces (*F/R*) as a function of distance of separation (*D*) between two silica surfaces in an aqueous solution containing 20 mM KCl at pH ~ 8.0 at various AMAC-70 concentrations.

Inset shows force profiles on semilog plot. Open and filled symbols represent approach and separation, respectively. Keys: (□) 0; (△, ▲) 2; (▼, ▽) 5.0; (♦, ◇) 10.0; and (●, ○) 50.0 ppm AMAC-70.

flocculation test is consistent with the more stretched polymer chains of AMAC-70 than those of AMAC-40 because of higher charge density of AMAC-70.

The settling results, in general, are in good agreement with force–distance data, even though we find no direct correspondence with regard to polymer concentrations. As described in the force–distance results section, there is no sign of bridging interactions in the presence of AMAC-15 for the entire concentration range. Bridging interactions, however, are evident in the presence of AMAC-40 and AMAC-70 at 5 and 10 ppm levels. It can be also noticed that the range and magnitude of bridging interactions predominate with the high charge density AMAC-70. A similar trend can be observed in the settling data.

Discussion

As shown in Figure 9, silica–silica interaction is a strong function of polymer charge density and concentration. The low charge density polymer acts as a dispersant at this experimental condition of 20 mM KCl at pH ~ 8.0, thereby resulting in purely repulsive force profiles on both approach and retraction, as was shown in Figure 4. The medium and high charge density polymers, however, could act as either flocculants or dispersants, depending on their concentration level. As shown in Figures 5 and 6, these polymers induce an adhesive bridging force at low concentrations and a purely repulsive force profile at higher concentrations. Similar conclusions can be drawn from silica flocculation tests shown in Figures 7 and 8. Using

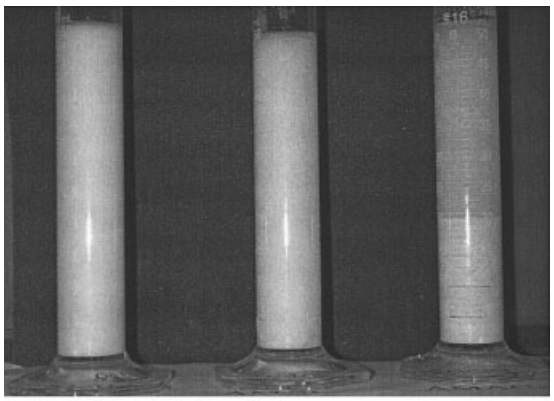

Figure 7. Silica dispersions (4.8%, w/w) in the presence of polymers of three different charge densities at 20 ppm level taken after 10 min of settling time.

The polymer charge densities are shown beneath the cylinders. See text for details.

mean-field models, Chatellier and Joanny (1996) studied the surface forces between similarly charged surfaces in polyelectrolyte solutions of different bulk concentrations. They predicted the transformation of surface forces from a long-range attractive force to a purely repulsive force with increasing polymer bulk concentration. Our observations are consistent with these theoretical predictions: the disappearance of bridging interactions with increasing polymer concentration, especially in the case of a high charge density polymer. It is interesting to note how the polymer charge density influences the surface interactions depending on the added polymer concentration. The effects of polymer charge density and polymer concentration on silica surface interactions in aqueous solutions are evident. In the following sections, we discuss major

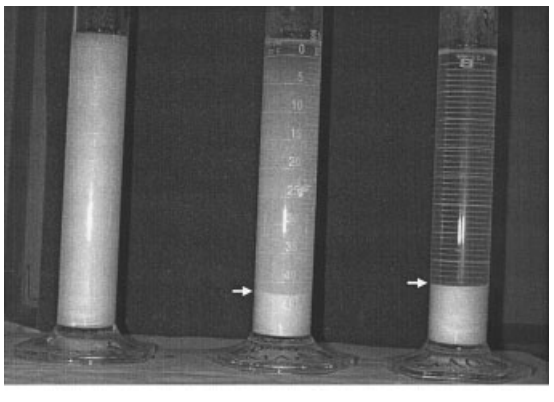

Figure 8. Silica dispersions (4.8%, w/w) in the presence of polymers of three different charge densities at 20 ppm level taken after overnight settling time.

The polymer charge densities are shown beneath the cylinders. See text for details.

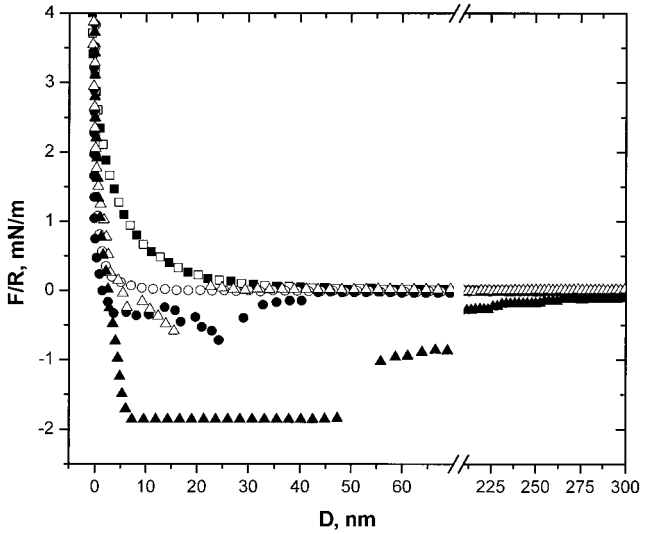

Figure 9. Comparison of measured forces between two silica surfaces in an aqueous solution containing 20 mM KCl at pH ~ 8.0 with 5.0 ppm polymer concentration.

Open and filled symbols represent approach and retraction, respectively. Keys: (□, ■) AMAC-15; (△, ▲) AMAC-40; (○, ●) AMAC-70.

results in conjunction with currently available polyelectrolyte theories on colloidal forces.

Bridging adhesion and polymer charge density

Figure 9 features the effects of polymer charge density on silica–silica surface interaction at 5 ppm. At this particular polymer concentration, the low charge density polymer causes a purely repulsive interaction, the medium density polymer causes a very small repulsive force on approach but an adhesive bridging interaction as surfaces retract, and the high charge density polymer causes an attractive bridging force as the surfaces approach and a huge adhesive bridging force on surface separation. The low charge density copolymer (15%), with the highest acrylamide content, gives rise to a very strong adsorption or high surface coverage, which eventually leads to purely repulsive force even at the low polymer concentration. The medium (40%) and high charge (70%) density copolymers, however, cause only a partial coverage at the 5 ppm concentration level and subsequently induce an adhesive bridging force. As one might observe, the adhesive bridging interaction is dominant with the high charge density polymer. In this case, the data suggest that the coverage of the surface by the polymer is partial. Although there is a layer of polymer on two surfaces, there are still some free surface sites available for polymer adsorption. For this reason, as the surfaces approach each other, there ought to be a bridging effect where the dangling tails of the polymers on one surface can contact and be adsorbed onto the other surface, thus potentially exerting an attractive influence on it. It was rare to note a jump-in in these experiments, although we did observe such a jump-in for high charge density polymer. However, on separation of the surfaces, a strong and long-ranged adhesion force was observed. The range of this attraction is very large, about 240 nm, and

thus it appears that on separation the polymer chain is being pulled off. To explain this, the length scales to be considered here include the mean square end-to-end distance ($\langle R_0^2 \rangle$) and the fully extended chain length (R_{FL}). Note that the predicted values of $\langle R_0^2 \rangle$ and R_{FL} are found to be 58 and 635 nm, respectively (see Table 1). While the polymer chain is being pulled off as the surfaces being separated, the chain could be perturbed from its equilibrium conformation (which corresponds to $\langle R_0^2 \rangle$), and therefore could have a size anywhere between 58 and 635 nm. The measured range of adhesive bridging interaction (that is, $\sim$ 240 nm) is justifiable in this respect.

Several theoretical treatises describe the effects of polymer charge density on surface interactions. One of the approaches is the continuum model, where the concentrations of the different species are taken to be continuous functions of the spatial coordinates. The mean-field equations of state were determined by solving two differential equations for the polymer concentration and the electrostatic potential derived using a variational procedure. Podgornik (1991, 1992) used a similar formalism to calculate intersurface forces, where the nonlinear excluded volume interaction between the monomers was not considered. Using these self-consistent field models, Podgronik predicted the transformation of force profiles from an attractive regime to a purely repulsive regime with an increase in l/k^{-1} values, where l is the actual distance between charges along the polymer chain and k^{-1} is the Debye screening length. Note that in our set of experiments, polymers of different l values were used while added salt (therefore k^{-1}) kept constant. Further, Borukhove et al. (1999) used a similar mean-field approach, but implicitly assuming that the polymer chain conformation remains Gaussian (that is, ignoring local stiffness of the chain). They predicted weakening of attractive force with decreasing polymer charge density. Consequently, the reduction in polymer charge density turns the colloidal forces from an attractive to a repulsive regime, depending on the added salt concentration. Podgornik also obtained an analytical expression that describes the bridging force as an exponentially decaying one. We did not observe any exponentially attractive bridging force in our experiments, although we did observe an attractive force regime for high charge density and adhesive bridging interaction in both medium and high charge density polymers.

Electrosteric interactions and polymer charge density

Figure 10 features the effects of polymer charge density on silica–silica surface interaction at a higher added polyelectrolyte concentration (50 ppm). All three charge density polymers give purely repulsive force in both approach and retraction, where the range and magnitude of repulsive force decrease significantly with increasing charge density. In the case of low charge density, the range of interaction extends up to about $2.4D_f$, suggesting significantly higher adsorbed polymers, whereas in the case of medium and high charge densities, the range of interaction is about $0.4D_f$.

The experimentally measured total range of interaction (R_I) decreases with increasing polymer charge density (f_p) with a power-law dependency:

$$R_I \propto f_p^{-0.97} \tag{7}$$

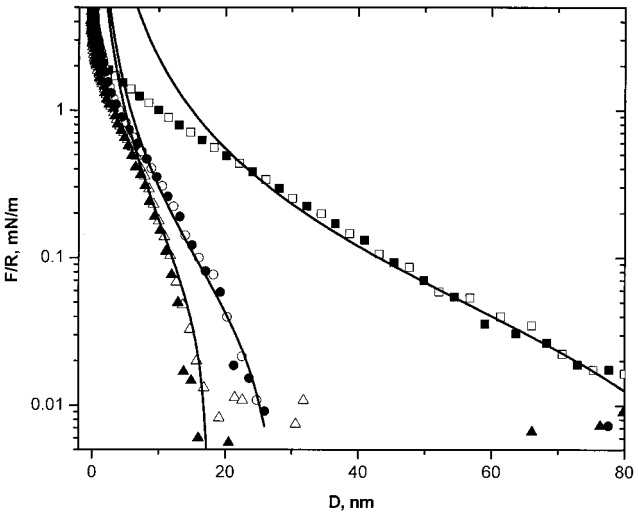

Figure 10. Comparison of measured forces between two silica surfaces in an aqueous solution containing 20 mM KCl at pH $\sim$ 8.0 at 50.0 ppm polymer concentration.

Open and filled symbols represent approach and separation respectively. Keys: (□, ■) AMAC-15; (○, ●) AMAC-70; (△, ▲) AMAC-70. Solid lines represent mean-field model fits according to Eq. 10. See text for details.

The total interaction ranges show a strong dependency on polymer charge density. For the low charge density case, 85% of its monomer units contain the amide group, which may interact with the silica substrate through hydrogen bonding. At the same time, because of its low acrylic content (15%), inter- and intrachain electrostatic interactions among the chains are low. Both these conditions, which are associated with the low charge density, favor strong adsorption. On the other hand, with medium and high charge density polymers, inter- and intrachain electrostatic interactions among the chains are high and at the same time they have low amide content. These factors limit the surface coverage, although the coverage is sufficient to provide adhesive bridging interactions.

Considering the system characteristics, the forces are clearly a combination of steric and electrostatic interactions. There are few theoretical attempts to describe electrosteric interactions and their dependency on polymer charge densities. To quantitatively explain these measured interactions, we follow here the work of Podgornik (1991). As outlined above, using self-consistent field (SCF) equations, Podgornik (1991) described similar systems, where long polyelectrolyte chains are confined between two charged macroscopic surfaces. The author obtained an analytical solution for the surface pressure. Podgornik quantified surface pressure (or interaction force) between two opposing surfaces as a function of separation distance (D) solely in terms of steric exclusion of charged polymer segments (bimodal distribution) as

$$\Pi(D) \approx \frac{\sigma^2}{\varepsilon\varepsilon_0}\left\{\left(\frac{\pi}{2}\right)^2\left[\frac{kT\varepsilon\varepsilon_0}{6\sigma\left(\frac{\tau}{l^2}\right)}\right]\frac{1}{D^3}+\frac{1}{4}\right\} \tag{8}$$

Here σ is the surface charge density of surface, ε_0 is the permittivity, ε is the dielectric constant of the medium, k is the

Boltzmann constant, T is the absolute temperature, τ is the net charge carried by each ionic group, and l is the distance between the charges along the polyelectrolyte chains. Upon integration of this equation and using Derjaguin approximation (Cappella and Deitler, 1999), the following equation of interaction energy between the two opposing polyelectrolyte surfaces positioned in sphere–flat surface geometry was obtained:

$$\left[\frac{F(D)}{R}\right] = -2\pi\int_{2L}^{D}\Pi(D')dD' = \frac{2\pi\sigma^2}{\varepsilon\varepsilon_0} \times \left\{\left(\frac{\pi}{2}\right)^2\left[\frac{kT\varepsilon\varepsilon_0}{6\sigma\left(\frac{\tau}{l^2}\right)}\right]\left(\frac{1}{2}\right)\left[\frac{1}{D^2}-\frac{1}{(2L)^2}\right]+\frac{1}{4}(L-D)\right\} \quad (9)$$

where L is the steric (polymer) layer thickness near the surface. Considering the system characteristics, the parameters ε_0, ε, k, T, and τ are essentially the same for all the polymers used in this study. The parameters that vary with polymer charge density are σ, l, and $2L$. Note that the surface charge density depends on the net counterion concentration in the system. The addition of polyelectrolytes, depending on their charge densities, would change the net counterion concentration. For instance, with the addition of high charge density polyelectrolyte, there would be more H^+ ions that would further screen the silica surfaces. One may write the above equation, in a simpler form, as

$$\left[\frac{F(D)}{R}\right] \sim \sigma^2\left\{\frac{1}{\sigma\left(\frac{1}{l^2}\right)}\left[\frac{1}{D^2}-\frac{1}{(2L)^2}\right]+\frac{1}{4}(L-D)\right\} \quad (10)$$

An attempt was made to describe the measured repulsive forces with Eq. 10. Reasonable fits can be obtained (Figure 10) with the steric (polymer) layer thickness (L), the distance between charges (l), and the surface charge density (σ) as adjustable parameters. The best-fit parameters are given in Table 2. Note that the reduction of surface charge density (σ) of bare silica with an increase in polymer charge density is conceivable because the use of high charge density polymer supplies more counterions (H^+ ions in this case), consequently reducing the surface charge density. A constant numerical prefactor of 800 is used. The fits for the short-ranged interactions, which are obviously of steric origin, deviate at shorter ranges. The discrepancy between the model and experimental data is evident, especially in the region of strong compression (small distance of separation) where the measured forces are shallower than the predicted force. Murat and Grest (1996) predicted using molecular dynamics simulation that splaying of the polymer chains underneath the tip can result in shallower profiles in similar AFM force measurement configurations. Overney et al. (1996) observed similar deviations between the AFM force profiles and SCF theories in the case of neutral polymers.

Table 2. Dimensions of Polymer Chains and Their Aggregates Determined by the Extrapolation of Dynamic Light Scattering Data in the Regime below 3.0 g/L to Zero Copolymer Concentration*

Copolymer	D_f (nm)	D_s (nm)
AMAC-15	34	285
AMAC-40	48	580
AMAC-70	—	—

*Note that the CONTIN analysis of sample AMAC-70 failed despite several attempts.

Table 3. Mean-Field Model–Fit Parameters According to Eq. 10*

Copolymer	σ (C/m^2)	L (nm)	l (nm)
AMAC-15	0.0051	45.0	7.56
AMAC-40	0.0048	13.0	3.02
AMAC-70	0.0046	8.8	2.67

*See Figure 10.

The proposed mean-field model (Table 3) can fairly well describe measured surface interactions in the presence of polyelectrolytes of different charge densities. Because the fits are based on three adjustable parameters, we will not consider these fitted values L, l, and σ as "real values." Nevertheless, one may infer the following from the fits. The confined polymer layer thickness (L) near the wall varies with polymer charge densities (f_p) as (Figure 11)

$$L \sim \frac{1}{f_P} \quad (11)$$

Such a relationship would mean that the low charge density polymer (chains with low f_p and higher l values) tends to form a thicker adsorbed layer (higher L values) that eventually gives rise to a long-range electrosteric repulsive force. Conversely, the medium and high charge density polymers (chains with high f_p and low l values) tend to form thin layers. This trend is also predicted from the mean-field lattice model calculations (Linse, 1996).

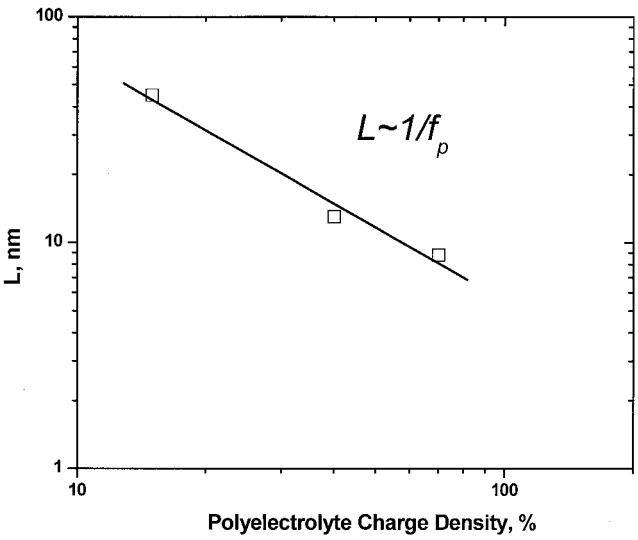

Figure 11. Fitted layer thickness (L) vs. polymer charge density.

Summary and Conclusions

The effects of polymer charge density on surface interactions between similarly charged silica surfaces were investigated using an atomic force microscope. Copolymers of acrylamide and acrylic acid of three different charge densities (f_p) of 15, 40, and 70% were used. The dynamic light-scattering technique was used to obtain the dimensional characteristics of these polymer solutions. Flocculation tests were performed to understand flocculation characteristics from the measured force profiles. The following conclusions can be drawn from this study:

(1) At 20 mM KCl and pH $\sim$ 8.0, the low charge density copolymer (f_p = 15%) adsorbs strongly onto silica surfaces, causing purely repulsive forces between the silica surfaces irrespective of the added polymer concentration.

(2) Under similar conditions, the medium (f_p = 40%) and high charge density copolymers (f_p = 70%) cause adhesive bridging attraction at low polymer concentration, but purely repulsive force at higher polymer concentrations. The range of this repulsive force, however, is significantly smaller than that measured for the low charge density polymer. The medium and high charge density copolymers exhibit nearly identical behavior in controlling the intersurface forces, although the forces are different with respect to magnitude.

(3) The flocculation tests follow the same trend as that of force–distance data, where a complete, a partial, and no flocculation were observed with high, medium, and low charge density polymers, respectively.

(4) In all these cases, the range of surface interactions is comparable to polymer chain dimensions that correspond to fast diffusion process (individual chains) obtained from dynamic light scattering.

(5) Mean-field models proposed for charged polymers can qualitatively explain both the dependency of bridging interactions on polymer charge density and the dependency of force–distance profiles on added polymer concentrations.

(6) A mean-field model can quantitatively account for the measured electrosteric interactions and their dependency on polymer charge density. The quantitative analysis suggests an inverse relationship between adsorbed polymer layer thickness and polymer charge density ($L \sim 1/f_p$).

Acknowledgments

Financial support from NSERC (Syncrude Industrial Research in Oil Sands Engineering) is greatly appreciated. J.F.G., "Chargé de Recherches" by the Belgian National Foundation for Scientific Research (F.N.R.S.), thanks the European Science Foundation SUPERNET program. J.F.G. and R.J. are very much indebted to the "Services Fédéraux des Affaires Scientifiques, Techniques et Culturelles" for financial support in the frame of the "Pôles d'attraction Interuniversitaires V/03: Supramolecular Chemistry and Supramolecular Catalysis."

Literature Cited

Abraham, T., "Effects of Divalent Salt on Adsorption Kinetics of a Hydrophobically Modified Polyelectrolyte at the Neutral Surface–Aqueous Solution Interface," *Polymer*, **43**, 849 (2002).

Abraham, T., D. Christendat, K. Karan, Z. Xu, and J. Masliyah, "Asphaltene–Silica Interactions in Aqueous Solutions: Direct Force Measurements Combined with Electrokinetic Studies," *Ind. Eng. Chem. Res.*, **41**, 2170 (2002).

Abraham, T., S. Giasson, J. F. Gohy, and R. Jérôme, "Direct Measurements of Interactions between Hydrophobically Anchored Strongly Charged Polyelectrolyte Brushes," *Langmuir*, **16**, 4246 (2000).

Abraham, T., A. Kumpulainen, Z. Xu, M. Rutland, P. M. Claesson, and J. Masliyah, "Polyelectrolyte Mediated Interaction between Similarly Charged Surfaces: Role of Divalent Counterions in Tuning the Surface Forces," *Langmuir*, **17**, 8321 (2001).

Attia, Y. A., *Flocculation in Biotechnology and Separation Systems*, Elsevier, Amsterdam (1987).

Biggs, S., "Steric and Bridging Forces between Surfaces Bearing Adsorbed Polymer: An Atomic Force Microscopy Study," *Langmuir*, **11**, 156 (1995).

Borukhov, I., D. Andelman, and H. Orland, "Effects of Polyelectrolyte Adsorption on Intercolloidal Forces," *J. Phys. Chem. B.*, **103**, 5042 (1999) [and references therein].

Cappella, B., and G. Deitler, "Force–Distance Curves by Atomic Force Microscopy," *Surf. Sci. Rep.*, **34**, 1 (1999).

Dahlgren, M. A. G., "Effects of Counterion Valency and Ionic Strength on Polyelectrolyte Adsorption," *Langmuir*, **10**, 1580 (1994).

Dahlgren, M. A. G., A. Waltermo, E. Blomberg, P. M. Claesson, L. Sjostrom, T. Akkesson, and B. Jonsson, "Salt Effects on the Interaction between Adsorbed Cationic Polyelectrolyte Layers," *J. Phys. Chem.*, **97**, 11769 (1993).

De Gennes, P. G., "Polymers at Interfaces; A Simplified View," *Adv. Colloid Interface Sci.*, **27**, 189 (1987)).

Ducker, W. A., T. J. Senden, and R. M. Pashley, "Direct Measurement of Colloidal Forces Using an Atomic Force Microscope," *Nature*, **353**, 239 (1991).

Farinato, R. S., Y. S. Huang, and P. Hawkins, *Colloid–Polymer Interactions*, R. S. Farinato and P. L. Dubin, Eds., Wiley–Interscience, New York, Chapter 1, p. 3 (1999).

Fleer, G. J., M. A. Stuart, J. M. H. M. Scheutjens, T. Cosgrove, and B. Vincent, *Polymers at Interface*, Chapman & Hall, London (1993).

Förster, S., M. Schmidt, and M. Antonietti, "Static and Dynamic Light Scattering by Aqueous Polyelectrolyte Solutions: Effects of Molecular Weight, Charge Density and Added Salt," *Polymer*, **31**, 781 (1990).

Israelachvili, J. N., *Intermolecular and Surface Forces*, 2nd Edition, Academic Press, London, Chapter 12 (1992a).

Israelachvili, J. N., *Intermolecular and Surface Forces*, 2nd Edition, Academic Press, London, Chapter 14 (1992b).

Joanny, J. F., and X. Chatellier, "Adsorption of Polyelctrolyte Solutions on Surfaces; A Debye–Huckel Therory," *J. Phys. II Fr.*, **6**, 1667 (1996).

Joanny, J. F., and X. Chatellier, "Adsorption of Gaussian Random Copolymer Chain at an Interface," *Eur. Phys. E.*, **1**, 9 (2000).

Kamiyama, Y., and J. Israelachvili, "Effects of pH and Salt on the Adsorption and Interactions of an Amphoteric Polyelectrolyte," *Macromolecules*, **25**, 5081 (1992).

Kelley, T. W., P. A. Schorr, D. J. Kristin, M. Tirrell, and C. D. Frisbie, "Direct Force Measurements at Polymer Brush Surfaces by Atomic Force Microscopy," *Macromolecules*, **31**, 4297 (1998).

Kujawa, P., J. M. Rosiak, J. Selb, and F. Candau, "Micellar Synthesis and Properties of Hydrophobically Associating Polyampholytes," *Macromol. Chem. Phys.*, **202**, 1384 (2001).

Linse, P., "Adsorption of Weakly Charged Polyelectrolytes at Oppositely Charged Surfaces," *Macromolecules*, **29**, 326 (1996).

Lowack, K., and C. A. Helm, "Molecular Mechanisms Controlling the Self-Assembly Process of Polyelectrolyte Multilayers," *Macromolecules*, **31**, 823 (1998).

Lyklema, J., *Fundamentals of Interface and Colloid Science*, Vol. II, Chapter 5, Academic Press, London (1995).

Milner, S. T., "Polymer Brushes," *Science* **251**, 905 (1991).

Murat, M., and G. Grest, "Molecular Dynamics Simulations of the Force between a Polymer Brush and an AFM Tip," *Macromolecules*, **29**, 8282 (1996).

Osterberg, M., J. Laine, P. Stenius, A. Kumpulainen, and P. M. Claesson, "Forces between Xylan-Coated Surfaces: Effect of Polymer Charge Density and Background Electrolyte," *J. Colloid Interface Sci.*, **242**, 59 (2001).

Overney, R. M., D. P. Leta, C. F. Pictroski, M. H. Rafailovich, Y. Liu, J. Quinn, J. Sokolov, A. Eisenberg, and G. Overney, "Compliance Measurements of Confined Polystyrene Solutions by Atomic Force Microscopy," *Phys. Rev. Lett.*, **76**, 1272 (1996).

Pincus, P., "Colloid Stabilization with Grafted Polyelectrolytes," *Macromolecules*, **24**, 2912 (1991).

Podgornik, R., "Electrostatlc Forces between Charged Surfaces in the Presence of a Polyelectrolyte Chain," *J. Phys. Chem.*, **95**, 5249 (1991).

Podgornik, R., "Self-Consistent-Field Theory for Confined Polyelectrolyte Chains," *J. Phys. Chem.*, **96**, 886 (1992).
Podgornik, R., T. Akesson, and B. Jonsson, "Colloidal Interactions Mediated via Polyelectrolytes," *J. Chem. Phys.*, **102,** 9423 (1995).
Provencher, S. W., "Inverse Problems in Polymer Characterization—Direct Analysis of Polydispersity with Photon Correlation Spectroscopy," *Macromol. Chem.*, **180**, 201 (1979).
Shubin, V., and P. Linse, "Self-Consistent-Field Modeling of Polyelectrolyte Adsorption on Charge-Regulating Surfaces," *Macromolecules*, **30**, 5944 (1998).
Texter, J., and M. Tirrell, "Chemical Processing by Self-Assembly," *AIChE J.*, **47**, 1706 (2001).
Verwey, E. J. W., and J. Th. G. Overbeek, *Theory of Stability of Lyophobic Colloids*, Elsevier, Amsterdam (1948).
Zhulina, E. B., and O. V. Borisov, "Structure and Interaction of Weakly Charged Polyelectrolyte Brushes: Self-Consistent Field Theory," *J. Chem. Phys.*, **107**, 5952 (1997).

Manuscript received May 27, 2003, and revision received Jan. 26, 2004.